Communication

Unidirectional Growth of Single-Walled Carbon Nanotubes

Naoki Ishigami, Hiroki Ago, Tetsushi Nishi, Ken-ichi Ikeda, Masaharu Tsuji, Tatsuya Ikuta, and Koji Takahashi

J. Am. Chem. Soc., **2008**, 130 (51), 17264-17265 • DOI: 10.1021/ja8080549 • Publication Date (Web): 03 December 2008

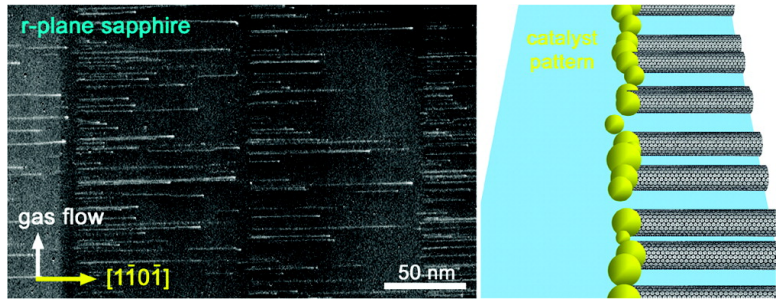

More About This Article

Additional resources and features associated with this article are available within the HTML version:

- Supporting Information
- Access to high resolution figures
- Links to articles and content related to this article
- Copyright permission to reproduce figures and/or text from this article

View the Full Text HTML

J|A|C|S
COMMUNICATIONS

Published on Web 12/03/2008

Unidirectional Growth of Single-Walled Carbon Nanotubes

Naoki Ishigami, Hiroki Ago,* Tetsushi Nishi, Ken-ichi Ikeda, Masaharu Tsuji, Tatsuya Ikuta, and Koji Takahashi

Graduate School of Engineering Sciences and Institute for Materials Chemistry and Engineering, Kyushu University, Kasuga, Fukuoka 816-8580, PRESTO, Japan Science and Technology Agency (JST), Kawaguchi, Saitama 332-0012, and Graduate School of Engineering, Kyushu University, Fukuoka 819-0395, Japan

Received October 13, 2008; E-mail: ago@cm.kyushu-u.ac.jp

Single-walled carbon nanotubes (SWNTs) have excellent electronic and physical properties, which make them attractive building blocks for nanoelectronics.[1] Directional control of SWNTs on a substrate is an essential step for the fabrication of high-performance integrated devices. Horizontally aligned SWNTs have been achieved by chemical vapor deposition (CVD) using single-crystal substrates, on which SWNTs grow along either atomic steps[2−4] (step-templated growth) or anisotropic surface atomic arrangements[4−7] (lattice-oriented growth). The lattice-oriented growth was observed on a-plane ($11\bar{2}0$) and r-plane ($1\bar{1}02$) sapphire (α-Al_2O_3)[5,6] and ST-cut quartz (SiO_2)[7,8] substrates, and these surfaces offer dense and highly aligned arrays of SWNTs. Recently, we observed that the crystalline surface affects not only the SWNT growth direction but also the diameter and chirality distribution of SWNTs.[9] This suggests a strong influence of the crystalline planes on the nanotube structure. On single-crystal surfaces, the patterning of a transition metal catalyst is effective to synthesize the high-density array of long SWNTs. The patterning maintains the clean substrate surface, thus preventing growth termination or misalignment due to the contaminated catalyst.[10−12] Generally, the aligned SWNTs grown from the catalyst pattern extend to both sides of the pattern.[10,11] Herein we achieved the unidirectional growth of SWNTs on an r-plane sapphire, where the SWNTs extend to only one side of the catalyst pattern without any external forces, such as gas flow and electric field. This unique growth mode is explained by the anisotropy in the surface atomic arrangement of the r-plane sapphire. Our finding offers a new method to control the direction as well as orientation and possible integration into advanced nanotube architectures.

The stripe pattern of a catalyst was made by photolithography on r- and a-plane sapphire and ST-cut quartz substrates. Two types of catalysts were studied for nanotube growth. The first was prepared by dip-coating a substrate into the aqueous solution of the Co−Mo salts, $Co(NO_3)_2 \cdot 6H_2O$ and $MoO_2(acac)_2$. The second was thin films of Fe or Co prepared by magnetron sputtering using the combinatorial masked deposition method proposed by Noda et al.;[13] a slit situated above the substrate made a gradual change in the film thickness over the whole area of a substrate. After lift-off, the substrate was subjected to thermal CVD in a flow of CH_4−H_2 mixed gases to synthesize SWNTs.[6,12]

Figure 1 shows scanning electron microscopy (SEM) and atomic force microscopy (AFM) images of aligned SWNTs grown from the stripe pattern of the Co−Mo salt catalyst on the r-plane sapphire. Most of the SWNTs extended only in the [$1\bar{1}0\bar{1}$] direction (we call it forward direction hereafter) and not in the opposite (backward) direction. This unidirectional growth is clearly seen in Figure 1b. The arrows indicate the nanotubes grown from the left catalyst line so that it is apparent that SWNTs were selectively extended to the forward direction. Note that the growth direction of the SWNTs

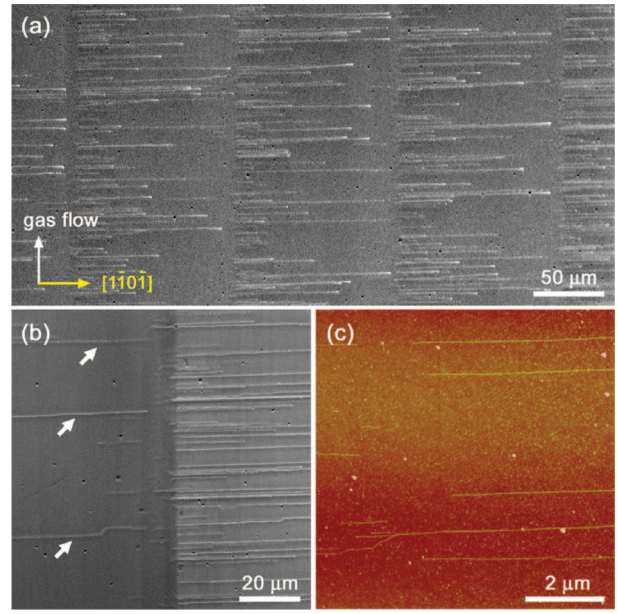

Figure 1. Unidirectional growth of SWNTs in [$1\bar{1}0\bar{1}$] direction from the Co−Mo salt-based catalyst stripe pattern on r-plane sapphire substrate; (a) low- and (b) high-magnification SEM images and (c) AFM image of the catalyst region.

was not influenced by the gas flow, because the slow gas flow and a slow heating rate were used. The AFM image (Figure 1c) showed that small metal nanoparticles were sparsely formed during the CVD process and that neither residual photoresist nor overloaded catalyst was present. This indicates that the observed unidirectional growth is not due to impurities. In contrast, no preferential growth was observed for the SWNTs grown on the a-plane sapphire (Supporting Information, Figure S3); the SWNTs grew in both the forward and backward directions equally from the catalyst line. The SWNTs aligned on an ST-cut quartz also showed no preferential growth direction (S3) consistent with the previous results.[10,11]

We examined the nanotube growth using a sputtered catalyst film with a gradient thickness distribution, as shown in Figures 2a and S4. Preferential growth in the forward direction was observed for both the Fe and Co films. This result suggests that the SWNT−substrate interaction is more important for unidirectional growth than the catalyst−substrate interaction, as is the case for the SWNT alignment.[11] The ratio of the forward SWNTs grown from the sputtered catalysts (r < 80%) was lower than that originated by the Co−Mo salt catalyst (96%). In the case of the sputtered catalyst, this ratio increased with decreasing film thickness; when the film thickness was decreased from 1.5 to 0.5 nm, the ratio increased from 65% to 74% for the Fe film and 68% to 77% for the Co film. The perfect unidirectional growth was not observed

10.1021/ja8080549 CCC: $40.75

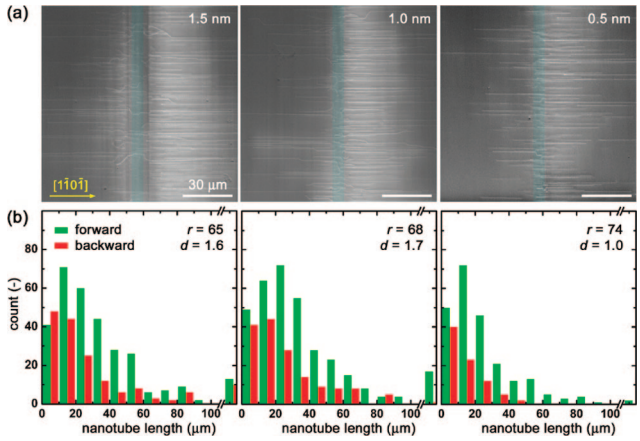

Figure 2. (a) SEM images of the aligned SWNTs grown from the Fe patterns with different film thicknesses. (b) Histograms of the length distribution of SWNTs. The SWNTs grown from a catalyst line with a length of 300 μm was counted. The r and d are the ratio of the forward SWNTs ($r = N_{\text{forward}}/(N_{\text{forward}} + N_{\text{backward}}) \times 100$) (%) and tube density ($d = (N_{\text{forward}} + N_{\text{backward}})/300\ \mu\text{m}$) ($\mu\text{m}^{-1}$), respectively.

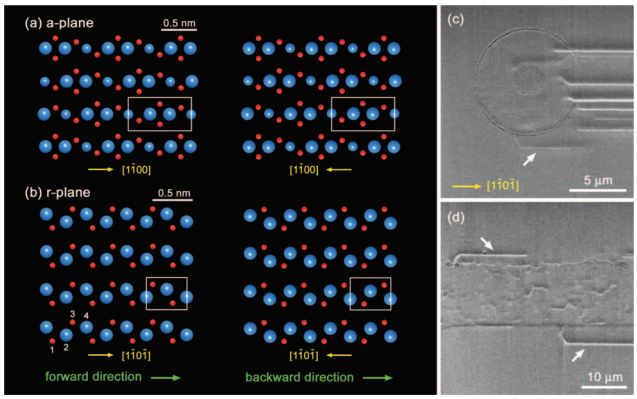

Figure 3. Surface atomic arrangements of sapphire (a) a- and (b) r-planes. Red and blue spheres represent Al and O atoms, respectively. The 180°-rotated arrangements are also shown. On the a-plane, the arrangements are equivalent to both directions, but they are different on the r-plane (squares are guides for eyes). The bond lengths are 0.186 (1Al−2O and 3Al−4O), 0.195 nm (2O−3Al) on the r-plane. SEM images of aligned SWNTs grown from the dot-shaped patterns (c) and a line pattern parallel to the [1$\bar{1}$0$\bar{1}$] direction (d) using the Co−Mo salt catalyst.

even for the very thin films with a thickness below 0.5 nm. The imperfect unidirectional SWNT growth for the sputtered catalyst may be originated from the damage of the surface atomic arrangement on the sapphire due to collision of the sputtered high-energy atoms and/or the inhomogeneous particle size distribution observed for the sputtered film (Figure S6). The length of the backward SWNTs was found to be relatively shorter than that of the forward nanotubes (Figure 2b), suggesting that nanotube growth in the forward direction is more favorable than the backward direction.

We speculate that the observed unidirectional SWNT growth is related to the surface atomic arrangement of the sapphire, because this was observed on the r-plane but not on the a-plane sapphire. Figure 3a,b illustrate the atomic models of the surfaces of the a- and r-plane sapphire. Reflecting the crystallographic orientation (Figure S7), the configuration of Al and O atoms on the a-plane sapphire has a point symmetry, while the r-plane lacks such symmetry. Therefore, we conclude that the anisotropy of the r-plane is the main reason for the observed unidirectional growth.

There are two possible mechanisms for the unidirectional growth. One possible explanation is the nucleation of a nanotube cap occurs dominantly to the forward direction in the very early stage of SWNT growth, assuming a base-growth model.[12,14,15] In this case, the nanotube chirality might be modulated by the sapphire surface, because the cap structure determines the SWNT chirality. Another possibility is that the extension of a SWNT in the forward direction is more energetically favored than the backward direction. For example, the nanotubes extending in the backward direction may have suffered from a larger frictional force due to geometric or electrostatic effects than the forward direction. The SEM images of the aligned SWNTs grown from the different patterns of the Co−Mo salt catalyst are displayed in Figure 3c,d. The SWNTs indicated by the arrows are bent in the [1$\bar{1}$0$\bar{1}$] direction soon after protruding from the catalyst pattern. These images suggest that there is a preferred direction for SWNTs to grow. Therefore, the latter mechanism may be more reasonable, but we should note that this also enhances the nucleation in the forward direction in the initial growth period. Further study is necessary to understand the mechanism and effect on the nanotube structure.

In summary, we achieved unidirectional growth of SWNTs by using the Co−Mo salt-based catalyst. The SWNTs were perfectly oriented in the [1$\bar{1}$0$\bar{1}$] direction without any external forces on the r-plane sapphire. The preferential growth of SWNTs is attributed to the asymmetric surface atomic arrangement of the r-plane. This unidirectional growth is expected to give further insight into the growth mechanism and structure control of SWNTs, leading to the fabrication of advanced architectures.

Acknowledgment. The work was supported by PRESTO-JST, a Grant-in-Aid for Scientific Research from the MEXT, and the Nanoelectronics Project of METI, Japan.

Supporting Information Available: Detailed experimental procedures and supplementary figures (S1−S7). This material is available free of charge via Internet at http://pubs.acs.org.

References

(1) Cao, Q.; Kim, H.; Pimparkar, N.; Kulkarni, J. P.; Wang, C.; Shim, M.; Roy, K.; Alam, M. A.; Rogers, J. A. *Nature* **2008**, *454*, 495.
(2) Ismach, A.; Segev, L.; Wachtel, E.; Joselevich, E. *Angew. Chem., Int. Ed.* **2004**, *43*, 6140.
(3) Kocabas, C.; Hur, S. H.; Gaur, A.; Meitl, M. A.; Shim, M.; Rogers, J. A. *Small* **2005**, *1*, 1110.
(4) Ago, H.; Imamoto, K.; Ishigami, N.; Ohdo, R.; Ikeda, K.; Tsuji, M. *Appl. Phys. Lett.* **2007**, *90*, 123112.
(5) (a) Han, S.; Liu, X.; Zhou, C. *J. Am. Chem. Soc.* **2005**, *127*, 5294. (b) Yu, Q.; Qin, G.; Li, H.; Xia, Z.; Nian, Y.; Pei, S. S. *J. Phys. Chem. B* **2006**, *110*, 22676.
(6) (a) Ago, H.; Nakamura, K.; Ikeda, K.; Uehara, N.; Ishigami, N.; Tsuji, M. *Chem. Phys. Lett.* **2005**, *408*, 433. (b) Ago, H.; Uehara, N.; Ikeda, K.; Ohdo, R.; Nakamura, K.; Tsuji, M. *Chem. Phys. Lett.* **2006**, *421*, 399.
(7) Kocabas, C.; Kang, S. J.; Ozel, T.; Shim, M.; Rogers, J. A. *J. Phys. Chem. C* **2007**, *111*, 17879.
(8) Yuan, D.; Ding, L.; Chu, H.; Feng, Y.; McNicholas, T. P.; Liu, J. *Nano. Lett.* **2008**, *8*, 2576.
(9) Ishigami, N.; Ago, H.; Imamoto, K.; Tsuji, M.; Iakoubovskii, K.; Minami, N. *J. Am. Chem. Soc.* **2008**, *130*, 9918.
(10) Kocabas, C.; Shim, M.; Rogers, J. A. *J. Am. Chem. Soc.* **2006**, *128*, 4540.
(11) Ding, L.; Yuan, D.; Liu, J. *J. Am. Chem. Soc.* **2008**, *130*, 5428.
(12) Ago, H.; Ishigami, N.; Yoshihara, N.; Imamoto, K.; Akita, S.; Ikeda, K.; Tsuji, M.; Ikuta, T.; Takahashi, K. *J. Phys. Chem. C* **2008**, *112*, 1735.
(13) Noda, S.; Sugime, H.; Osawa, T.; Tsuji, Y.; Chiashi, S.; Murakami, Y.; Maruyama, S. *Carbon* **2006**, *44*, 1414.
(14) Liu, X.; Ryu, K.; Badmaev, A.; Han, S.; Zhou, C. *J. Phys. Chem. C* **2008**, *112*, 15929.
(15) Rümmeli, M. H.; Schäffel, F.; Kramberger, C.; Gemming, T.; Bachmatiuk, A.; Kalenczuk, R. J.; Rellinghaus, B.; Büchner, B.; Pichler, T. *J. Am. Chem. Soc.* **2007**, *129*, 15772.

JA8080549